Electrochemical Nanotechnology

DOI: 10.1002/anie.200704144

Growth of Aligned TiO_2 Bamboo-Type Nanotubes and Highly Ordered Nanolace**

*Sergiu P. Albu, Doohun Kim, and Patrik Schmuki**

Synthesis of carbon nanotubes by Iijima in 1991[1] stimulated intense research activity worldwide due to the anticipated technological impact of this unique combination of material, directionality, and dimension that could be exploited to enhance a plethora of materials properties. In the following years the chemical synthesis of various non-carbon nanotubes, in particular transition metal oxide nanotubes such as TiO_2 (titanate) and V_2O_5 was achieved, mainly by using hydrothermal techniques.[2–5] More recently a simple, cheap, and straightforward approach was reported that leads to ordered TiO_2 nanotube arrays that grow self-aligned during anodization of Ti.[6] The layers can be grown with tube dimensions varying from a few micrometers in length up to several hundreds of micrometers, and with diameters varying from about 10 to 200 nm.[7–10] These layers of self-organized oxide nanotube structures, which are attached to the Ti substrate or suspended as membranes[11] have created significant interest due to their anticipated impact in various applications. In particular, the properties of the material have been tailored for solar-energy conversion with dye sensitization[12–14] or doping[15–18] and display applications with enhanced electrochromic switching.[19] Other reports focused on use as a photocatalyst[20,21] or in sensing,[22] and due to the high biocompatibility of TiO_2, interactions of biological cells with the tubular surface[23] or enhanced bone formation on the material[24] were studied.

These oxide nanotubes are grown by anodization of a Ti metal sheet in dilute fluoride electrolytes at a certain voltage for a given time. Typically the tube diameter is controlled by the applied anodization voltage,[10,25] and the length can be varied by means of the anodization time and by using different electrolytes. Anodization under constant-voltage conditions leads to an ordered layer consisting of a distinct morphology of smooth tubes with defined cylindrical or hexagonal cross section.[7,26]

Herein we show how novel morphologies such as bamboo-type reinforced nanotubes and two-dimensional (2D) nanolace sheets can be obtained if the anodization process is carried out under specific alternating-voltage (AV) conditions. Figure 1 shows an examples of smooth and bamboo-type structures.

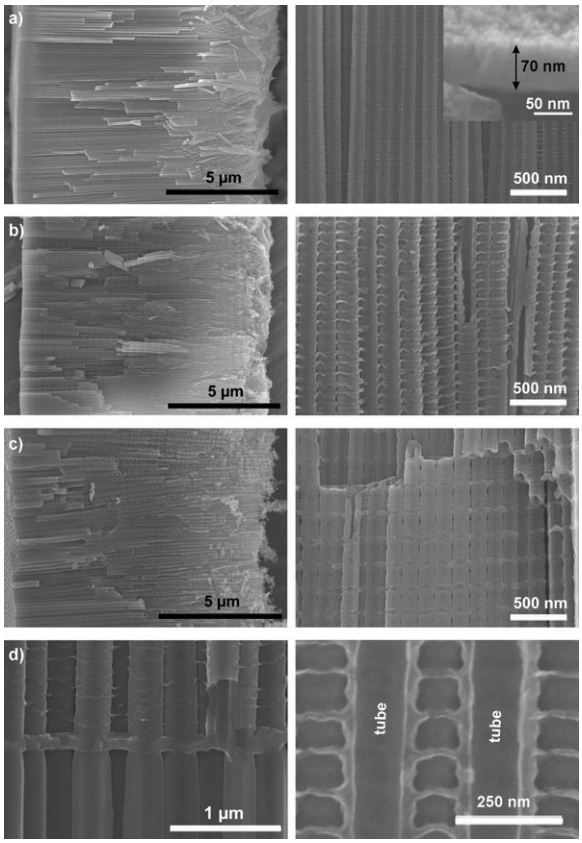

Figure 1. SEM images of anodically grown nanotube layers of 10-µm thickness. a) With smooth walls, grown under constant-voltage conditions (120 V). b) Bamboo-type tubes, grown under AV conditions, with a sequence of 1 min at 120 V and 5 min at 40 V. c) As in (b) but with an AV sequence of 2 min at 120 V and 5 min at 40 V. The left image shows the whole layer, and the right image a magnification of the tubes. The inset in Figure 1 a (right) shows the initial compact layer formed at short times (30 s) at 120 V. d) Higher magnification of the tube reinforcement; the right image shows a cross section through an opened bamboo structure.

The key to this approach is exploiting the fact that, during the initial stages of anodization, two fundamentally different oxide morphologies grow successively on the Ti surface. In the first stage, a compact anodic oxide is formed, and only after a certain period of time does the growth of ordered nanotubular structures take place. During the initial growth phase, pH and diffusion gradients are established that finally allow a tubular morphology to grow.[8,9] If this system is altered by a step to lower voltage, the concentration profiles will be adjusted to less steep gradients. Therefore, a subsequent step to the higher values will again lead to formation of an

[*] S. P. Albu, D. Kim, Prof. Dr. P. Schmuki
Department of Materials Science, WW4-LKO
University of Erlangen-Nuremberg
Martensstrasse 7, 91058 Erlangen (Germany)
Fax: (+49) 9131-852-7582
E-mail: schmuki@ww.uni-erlangen.de

[**] We acknowledge DFG for financial support. Hans Rollig and Martin Kolacyak are acknowledged for valuable technical help.

initiation layer. As a consequence, when the voltage is alternated between two formation voltages, tube growth and initiation can be established repeatedly.

Figure 1a shows a nanotube layer grown under constant-voltage conditions, at 120 V in an electrolyte consisting of 0.2 mol L^{-1} HF in ethylene glycol. After 2 h of anodization a very regular layer with a thickness of about 10 μm forms that consists of aligned, individual (separated) TiO_2 nanotubes with diameters of 150 nm. Important for the present work is that in the very first moments of anodization, that is, for anodization times of less than 1 min, a nontubular "compact" layer with a thickness of about 40–80 nm forms (Figure 1a, inset).

If the voltage is lowered to 40 V, the growth of the tubes slows down and, depending on the resulting conditions, may entirely stop. When the voltage is alternated between an upper level (120 V) and a lower level (here 40 V), and the holding time at the lower level is sufficiently long, a subsequent step to 120 V again leads to a compact initiation layer, and a bamboo type of structure can be grown (Figure 1b,d).

The spacing between the bamboo rings can be altered by means of the time for which the sample is held at 120 V, as shown in Figure 1b,c where the spacing was reduced from 200 to 70 nm by reducing the holding time. Figure 1d shows that the tubes are open on the inside after the ring-formation process. It is also apparent that the reinforcements do not lead to a change of inner tube diameter; instead, a continuous uniform channel is formed in each case.

The anodic current registered during the experiment under constant-voltage conditions or under AV conditions (Figure 2a) reveals details about the timescales of the different stages of the growth process and the corresponding morphologies (Figure 2b and c). Typical for all constant-voltage conditions is the sequence schematically shown in Figure 2c. After applying a voltage step in stage I, a compact oxide layer forms that hampers further ion transfer and thus is of self-limiting nature (under high-field conditions). As a result, the current drops exponentially with increasing layer thickness. Based on the electrochemical data in Figure 1a (the initial current decay at 120 V) and the data in Figure 2b (morphology and tube growth rate from SEM observations at 120 V), this initial phase lasts for around 30–60 s under the conditions established at 120 V. In the second stage, the layer is partially perforated by fluoride ion migration and accompanying oxide dissolution,[27] a fine porous layer forms, and the current increases. In the third stage the situation is stabilized, and regularly growing pores or tubes are formed. These growth stages are also apparent from the current response during AV stepping. By examining the details of a single current response, that is, a transient when stepping to 120 V, it is clear that it consists of two parts: the first, lasting about 30 s, can be ascribed to growth of compact oxide, and the second to tube growth.

The finding that for the first few pulses a different transient behavior is obtained than for later transients is likely due to the fact that a sufficiently long tube must be formed to make a steady-state diffusion-controlled mechanism operative. This is also supported by the results of Figure 2b, which

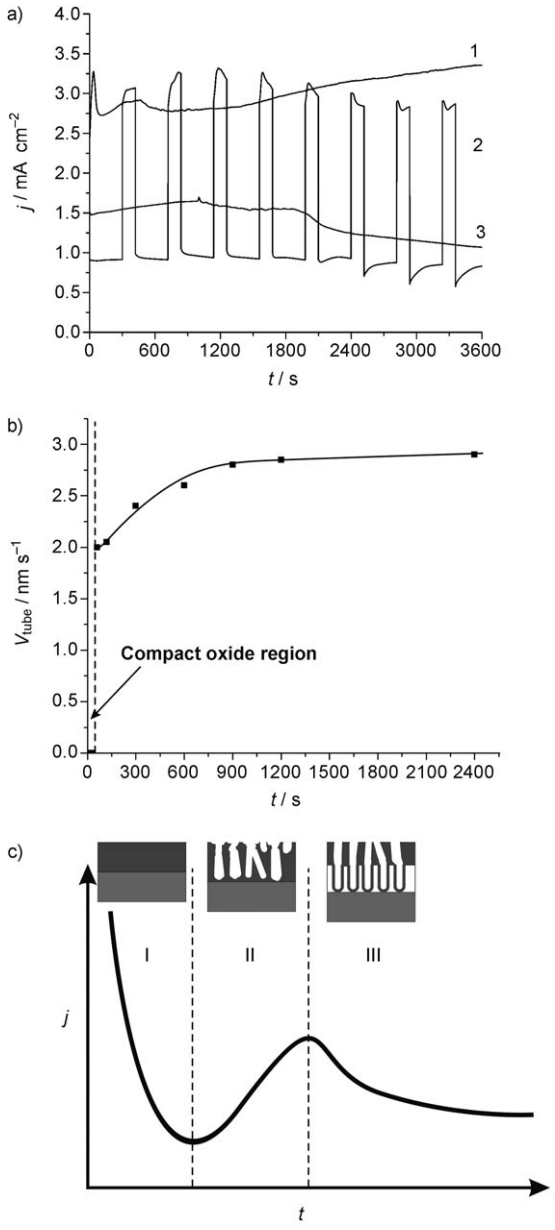

Figure 2. a) Current/time characteristics (j = current density) for constant-voltage anodization at 120 V (1), 40 V (3), and an AV sequence of 2 min at 120 V and 5 min at 40 V (2). b) Growth rate v_{tube} of initial compact oxide layer and nanotubes under constant-voltage conditions at 120 V. c) Typical current/time characteristics and corresponding growth stages during self-organization process. I: initial compact oxide, II: perforated, random tubular layer, III: self-organized tube growth.

provides the time dependence of the growth rate of the nanotubes at 120 V in constant-voltage anodization. The results show that even when the tube-growth regime has been established, the growth rate increases with time. This must be ascribed to the final profile in the local tube chemistry[8] and the according diffusion profile establishing a steady state at sufficient tube length.

Relatively slow diffusion processes mean that in AV anodization the tube growth rate is not linear after a voltage step to 120 V and an equilibration phase is observed until the

steady-state growth rate of tubes (maximum speed) is recovered.

In order to repeatedly produce bamboo rings in each step to 120 V, sufficient time for relaxation of the diffusion profile at the lower voltage must be allowed for (without completely shutting down the growth reaction). The maximum holding time at the lower voltage is determined by the incubation time at this voltage for initiation of actively growing tubes. At 40 V, the transition from the growth of a compact initiation layer to a nanotubular layer, as shown in Figure 3a, b, occurs at around 1800 s; this is also apparent in the maximum in the corresponding current/time curve in Figure 2a.

If anodization takes place for a longer time at the lower voltage, nanotubular features with a reduced diameter start to grow.[28,29] This can be exploited to grow a double-layer structure (Figure 3c and d). In this case branching of the main tube with a diameter of 150 nm into several (typically 2–3) smaller tubes of about 50 nm in diameter can be observed.

Interesting 2D nanogrid (nanolace) structures are obtained if voltage cycling is carried out for an extended period of time (Figure 4). We ascribed this finding to permanent chemical etching of the nanotube structure in the fluoride containing electrolyte: $TiO_2 + 6\,HF \rightarrow TiF_6^{2-} + 2\,H_2O + 2\,H^+$.

Therefore, the thinnest part of the tube wall formed at the higher voltage is etched off and the reinforced compact parts are left behind. This means that the outermost part of a reinforced tube layer will be exposed to the electrolyte for the longest time and the tube walls will be etched out first to form a first layer of nanolace. With increasing anodization time layer after layer is formed, stacked on each other as shown in Figure 4b. This additionally implies that the compact oxide has a lower chemical etching rate than the tube walls. Such an effect may be ascribed to "ageing" of the oxide[30,31] or the loss of field-influenced etching effects when the 2D layers are disconnected from the circuit at the moment the connecting tube structure is lost. Interestingly, detailed inspection of the lace morphology reveals that the original outer tube walls and

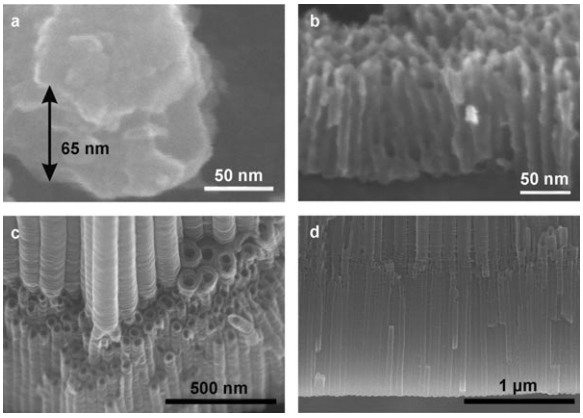

Figure 3. Morphology evolution at 40 V (a, b) and formation of two-diameter stack layer (c, d). a) Compact layer after 5 min of anodization. b) First tubes forming after 30 min of anodization. c) Tilted cross section of a double layer formed by one AV step, first at 120 V (6 h) and then at 40 V (2 h). d) Cross-section of the double-layer structure in (c).

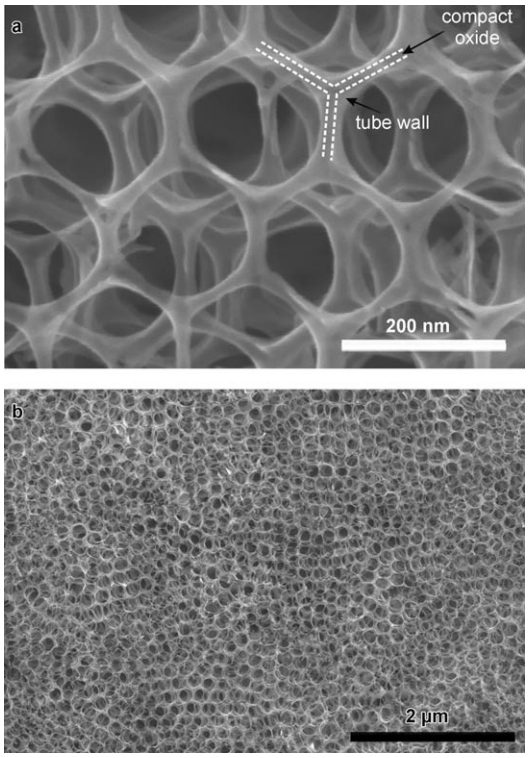

Figure 4. TiO_2 nanolace sheets formed by extended AV anodization with a sequence of 50 s at 120 V and 600 s at 0 V. a) Detailed view with indication of original tube walls and compact oxide formed by pulsing. b) Overview of layer surface area.

the space filled by the reinforcement layer can clearly be distinguished in SEM images. The structural features that remain have diameters down to 10 nm, which is already in the range for which the onset of quantum-size effects can be expected for TiO_2.[32] Moreover, the lace structure can extend over the entire sample surface (ca. 1 cm^2) with only very few local defects, that is, the structure has a very large lateral aspect ratio.

X-ray diffraction experiments on bamboo-tube and nanolace morphologies revealed an amorphous nature for the as-formed material. In both cases the structures could be crystallized to an anatase structure without losing structural integrity by annealing in air at 450 °C.

In summary, the present work shows that several new nanoscale TiO_2 morphologies can be produced by alternating-voltage anodization of Ti in fluoride-containing electrolytes under optimized conditions, as illustrated in Figure 5. By establishing conditions that lead to alternating growth of tubes and a compact layer, a regular tube structure with bamboolike features can be grown. These structural modulations of the nanotubes can be exploited to mechanically reinforce the nanostructure, or alternatively to optimize the volume filling of TiO_2 nanostructures, for example, in photoconversion applications. A second type of nanostructure, namely, a multidiameter stack of nanotubes, can be generated simply by adjusting the anodization times at different anodization voltages. In this case a layer of nanotubes of smaller diameter can be grown underneath a primary layer, with tubes that penetrate the bottom of the first tube layer.

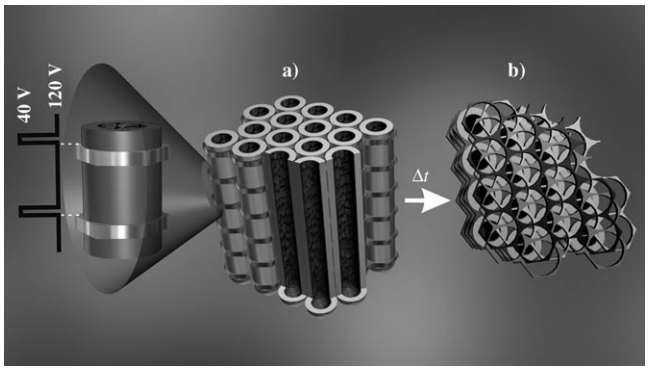

Figure 5. Illustration of the growth of TiO_2 bamboo-type and nanolace structures. a) Formation of bamboo ring by voltage steps. b) Formation of nanolace by side-wall etching (extended time in electrolyte).

The thickness of this second layer can be in the range of several micrometers depending on the anodization time. Such multilayer structures may have significant applications, for example, in size-selective reactive filtration, or the possibility to form two distinct layers might be exploited with regard to optical properties, such as in Bragg-stack structures.[33,34]

The third structure produced by AV anodization is a TiO_2 nanolace, a 2D sheet material with dimensions close to the size scale for which quantum size effects can be expected for TiO_2. Furthermore, such lace structures may be embedded in semiconductor nanocomposites to exploit the efficient electron-harvesting ability of TiO_2 in a system-penetrating scaffold.

Experimental Section

Titanium foils (0.1 mm, 99.6% purity, Advent Materials) were degreased prior to electrochemical experiments by sonication in acetone, 2-propanol, and methanol, subsequently rinsed with deionized (DI) water, and finally dried in a nitrogen stream. The samples were pressed together with a Cu plate against an O-ring in an electrochemical cell (leaving 1 cm^2 exposed to the electrolyte) and anodized in an organic electrolyte consisting of ethylene glycol (Riedel-de Haën, containing less than 0.2 wt% H_2O) with additions of 0.2 mol L^{-1} HF (40%, Merck) and 0.12 mol L^{-1} H_2O_2 (30%, Merck). Before use, the electrolyte was "aged" for 24 h at 120 V (60 mA h $L)^{-1}$.

For the electrochemical experiments, a Jaissle IMP 88 PC-200 high-voltage potentiostat (Jaissle Elektronik GmbH, Germany) controlled by a programmable voltage source that superimposed the AV signal was used. The voltages used were 120, 40, and 0 V; the holding time of the two voltages was varied.

A conventional three-electrode configuration with a platinum gauze as counterelectrode and a Haber–Luggin capillary with Ag/AgCl (1M KCl) as a reference electrode were used. All electrolytes were prepared from reagent-grade chemicals. A Hitachi FE-SEM S4800 scanning electron microscope was used for morphological and structural characterization of the TiO_2 nanotubular layers.

Received: September 7, 2007
Published online: January 29, 2008

Keywords: electrochemistry · nanostructures · nanotubes · self-organization · titanium

[1] S. Iijima, *Nature* **1991**, *354*, 56–58.
[2] P. Hoyer, *Adv. Mater.* **1996**, *8*, 857–859.
[3] T. Kasuga, M. Hiramatsu, A. Hoson, T. Sekino, K. Niihara, *Langmuir* **1998**, *14*, 3160–3163.
[4] F. Krumeich, H. J. Muhr, M. Niederberger, F. Bieri, B. Schnyder, R. Nesper, *J. Am. Chem. Soc.* **1999**, *121*, 8324–8331.
[5] X. Sun, Y. Li, *Chem. Eur. J.* **2003**, *9*, 2229–2238.
[6] V. Zwilling, M. Aucouturier, E. Darque-Ceretti, *Electrochim. Acta* **1999**, *45*, 921–929.
[7] S. P. Albu, A. Ghicov, J. M. Macak, P. Schmuki, *Phys. Status Solidi RRL* **2007**, *1*, R65–R67.
[8] J. M. Macak, H. Tsuchiya, P. Schmuki, *Angew. Chem.* **2005**, *117*, 2136–2139; *Angew. Chem. Int. Ed.* **2005**, *44*, 2100–2102.
[9] J. M. Macak, H. Tsuchiya, L. Taveira, S. Aldabergerova, P. Schmuki, *Angew. Chem.* **2005**, *117*, 7629–7632; *Angew. Chem. Int. Ed.* **2005**, *44*, 7463–7465.
[10] S. Bauer, S. Kleber, P. Schmuki, *Electrochem. Commun.* **2006**, *8*, 1321–1325.
[11] S. P. Albu, A. Ghicov, J. M. Macak, R. Hahn, P. Schmuki, *Nano Lett.* **2007**, *7*, 1286–1289.
[12] J. M. Macak, H. Tsuchiya, A. Ghicov, P. Schmuki, *Electrochem. Commun.* **2005**, *7*, 1133–1137.
[13] K. Zhu, N. R. Neale, A. Miedaner, A. J. Frank, *Nano Lett.* **2007**, *7*, 69–74.
[14] R. Hahn, T. Stergiopoulus, J. M. Macak, D. Tsoukleris, A. G. Kontos, S. P. Albu, D. Kim, A. Ghicov, J. Kunze, P. Falaras, P. Schmuki, *Phys. Status Solidi RRL* **2007**, *1*, 135–137.
[15] A. Ghicov, J. M. Macak, H. Tsuchiya, J. Kunze, V. Haeublein, L. Frey, P. Schmuki, *Nano Lett.* **2006**, *6*, 1080–1082.
[16] J. M. Macak, A. Ghicov, R. Hahn, H. Tsuchiya, P. Schmuki, *J. Mater. Res.* **2006**, *21*, 2824–2828.
[17] J. H. Park, S. Kim, A. J. Bard, *Nano Lett.* **2006**, *6*, 24–28.
[18] R. Hahn, A. Ghicov, J. Salonen, V.-P. Lehto, P. Schmuki, *Nanotechnology* **2007**, *18*, 105604.
[19] A. Ghicov, H. Tsuchiya, R. Hahn, J. M. Macak, A. G. Munoz, P. Schmuki, *Electrochem. Commun.* **2006**, *8*, 528–532.
[20] J. M. Macak, P. J. Barczuk, H. Tsuchiya, M. Z. Nowakowska, A. Ghicov, M. Chojak, S. Bauer, S. Virtanen, P. J. Kulesza, P. Schmuki, *Electrochem. Commun.* **2005**, *7*, 1417–1422.
[21] J. M. Macak, M. Zlamal, J. Krysa, P. Schmuki, *Small* **2007**, *3*, 300–304.
[22] O. K. Varghese, D. Gong, M. Paulose, K. G. Ong, C. A. Grimes, *Sens. Actuators B* **2003**, 93, 338–344.
[23] J. Park, S. Bauer, K. Von Mark, P. Schmuki, *Nano Lett.* **2007**, *7*, 1686–1691.
[24] H. Tsuchiya, J. M. Macak, L. Müller, J. Kunze, F. Müller, P. Greil, S. Virtanen, P. Schmuki, *J. Biomed. Mater. Res. Part A* **2006**, *77*, 534–541.
[25] H. Tsuchiya, J. M. Macak, A. Ghicov, P. Schmuki, *Small* **2006**, *2*, 888–891.
[26] J. M. Macak, S. P. Albu, P. Schmuki, *Phys. Status Solidi RRL* **2007**, *1*, 181–183.
[27] L. V. Taveira, J. M. Macak, H. Tsuchiya, L. F. P. Dick, P. Schmuki, *J. Electrochem. Soc.* **2005**, *152*, B405–B410.
[28] K. Yasuda, P. Schmuki, *Electrochem. Commun.* **2007**, *9*, 615–619.
[29] J. M. Macak, S. Albu, D. H. Kim, I. Paramasivam, S. Aldabergerova, P. Schmuki, *Electrochem. Solid-State Lett.* **2007**, *10*, K28–K31.
[30] T. Ohtsuka, T. Otsuki, *Corros. Sci.* **2003**, *45*, 1793–1801.
[31] J. Kunze, A. Seyeux, P. Schmuki, unpublished results.
[32] S. Balaji, Y. Djaoued, J. Robichaud, *J. Raman Spectrosc.* **2006**, *37*, 1416–1422.
[33] H. Tsuchiya, M. Hueppe, T. Djenizian, P. Schmuki, *Surf. Sci.* **2003**, *547*, 268–274.
[34] G. Vincent, *Appl. Phys. Lett.* **1994**, *64*, 2367–2369.

